

# In-medium chiral condensate beyond linear density approximation <sup>1</sup>

N. Kaiser, P. de Homont, and W. Weise

Physik Department, Technische Universität München, D-85747 Garching, Germany

## Abstract

In-medium chiral perturbation theory is used to calculate the density dependence of the quark condensate  $\langle\bar{q}q\rangle$ . The corrections beyond the linear density approximation are obtained by differentiating the interaction contributions to the energy per particle of isospin-symmetric nuclear matter with respect to the pion mass. Our calculation treats systematically the effects from one-pion exchange (with  $m_\pi$ -dependent vertex corrections), iterated  $1\pi$ -exchange, and irreducible  $2\pi$ -exchange including intermediate  $\Delta(1232)$ -isobar excitations, with Pauli-blocking corrections up to three-loop order. We find a strong and non-linear dependence of the “dropping” in-medium condensate on the actual value of the pion (or light quark) mass. In the chiral limit,  $m_\pi = 0$ , chiral restoration appears to be reached already at about 1.5 times normal nuclear matter density. By contrast, for the physical pion mass,  $m_\pi = 135$  MeV, the in-medium condensate stabilizes at about 60% of its vacuum value above that same density. Effects from  $2\pi$ -exchange with virtual  $\Delta(1232)$ -isobar excitations turn out to be crucial in generating such pronounced deviations from the linear density approximation above  $\rho_0$ . The hindered tendency towards chiral symmetry restoration provides a justification for using pions and nucleons as effective low-energy degrees of freedom at least up to twice nuclear matter density.

PACS: 12.38.Bx, 21.65.+f

Keywords: In-medium chiral condensate, long-range correlations in nuclear matter from one- and two-pion exchange.

## 1 Introduction and framework

The quark condensate  $|\langle 0|\bar{q}q|0\rangle|$  is an order parameter of spontaneous chiral symmetry breaking in QCD. With increasing temperature the quark condensate decreases (or “melts”). For low temperatures this effect can be systematically calculated in chiral perturbation theory. At three-loop order [1] the estimate  $T_c \simeq 190$  MeV for the critical temperature, where chiral symmetry will eventually be restored, has been found. This extrapolated value of  $T_c$  is remarkably consistent with  $T_c = (192 \pm 8)$  MeV [2] obtained in numerical simulations of full QCD on the lattice, although this result is still under debate. It has subsequently been criticized [3] with respect to the reliability of the continuum extrapolation performed in ref.[2]. In fact the QCD chiral “phase transition” is merely a non-singular cross-over, with the transition temperature (deduced from the peak of the chiral susceptibility) lying in the broad range  $T_c = (160 \pm 29)$  MeV according to ref.[3].

The chiral condensate  $|\langle\bar{q}q\rangle|$  drops also with increasing baryon density. Presently, it is not feasible to study this phenomenon rigorously in lattice simulations of QCD due to the problems arising from the complex-valued Euclidian Fermion determinant at non-zero baryon chemical potential. As an alternative, the density dependence of the quark condensate  $\langle\bar{q}q\rangle(\rho)$  can be extracted by exploiting the Feynman-Hellmann theorem applied to the chiral symmetry breaking quark mass term  $m_q \bar{q}q$  in the QCD Hamiltonian. The leading linear term in the

---

<sup>1</sup>Work supported in part by BMBF, GSI and by the DFG cluster of excellence: Origin and Structure of the Universe.

nucleon density  $\rho$  is then readily derived by differentiating the energy density of a nucleonic Fermi gas,  $\rho M_N + \mathcal{O}(\rho^{5/3})$ , with respect to the light quark mass  $m_q$ . This introduces the nucleon sigma-term  $\sigma_N = \langle N | m_q \bar{q}q | N \rangle = m_q \partial M_N / \partial m_q = (45 \pm 8) \text{ MeV}$  [4] as the driving term for the density evolution of the chiral condensate. Following this simple linear density approximation one would naively estimate that chiral symmetry gets restored at  $(2.5 - 3)\rho_0$ , with  $\rho_0 = 0.16 \text{ fm}^{-3}$  the nuclear matter saturation density.

Corrections beyond the linear density approximation arise from the nucleon-nucleon interactions which transform the nucleonic Fermi gas into a nuclear Fermi liquid. These corrections have been studied in one-boson exchange models of the NN-interaction combined with the relativistic Dirac-Brueckner approach to nuclear matter [5, 6]. Knowledge of the quark mass derivatives of the various meson masses and coupling constants is required in order to quantify the interaction effects on the in-medium condensate. For the vector and scalar bosons it has been assumed that their sigma-terms scale linearly with that of the nucleon, i.e.  $m_q \partial m_{V,S} / \partial m_q = \sigma_N m_{V,S} / M_N$ . In the further development it has been demonstrated in ref.[7] that the higher order corrections (in density) depend sensitively on the interpretation of the isoscalar scalar " $\sigma$ "-boson (which is responsible for the central NN-attraction in one-boson exchange models) and its substructure. Within modest variations of an unknown parameter  $0 \leq C_S \leq 1$  both an accelerated and a hindered tendency towards chiral restoration are possible. The way out of this dilemma is to replace the fictitious " $\sigma$ "-boson exchange by realistic two-pion exchange processes.

Because of the Goldstone boson nature of the pion with its characteristic mass relation,  $m_\pi^2 \sim m_q$ , the pion-exchange dynamics in nuclear matter plays a particularly important role for the in-medium quark condensate. A first step in this direction was made in ref.[8] where realistic saturation of nuclear matter could be obtained from the iteration of  $1\pi$ -exchange plus a short-range NN-contact interaction to second order. It was found that the pionic interaction effects (with well-known quark mass derivative) counteract the reduction of the condensate from the leading linear term in density. Actually, if one restricts oneself to the density region  $\rho \leq \rho_0 = 0.16 \text{ fm}^{-3}$ , then all existing calculations agree that the deviations from the linear density approximation are relatively small and practically get masked by the uncertainty of the empirical nucleon sigma-term,  $\sigma_N = (45 \pm 8) \text{ MeV}$ .

The chiral approach to nuclear matter has been extended and improved in refs.[9, 10] by systematically including effects from irreducible  $2\pi$ -exchange together with excitations of virtual  $\Delta(1232)$ -isobars. The physical motivation for such an extension is threefold. First, the spin-isospin-3/2  $\Delta(1232)$ -resonance is the most prominent feature of low-energy  $\pi N$ -scattering. Secondly, it is well known that the  $2\pi$ -exchange between nucleons with excitations of virtual  $\Delta$ -isobars generates the medium- and long-range components of the isoscalar central NN-attraction [11], which is simulated by the scalar " $\sigma$ "-boson in the one-boson exchange models. Thirdly, the delta-nucleon mass-splitting  $\Delta = 293 \text{ MeV}$  is of the same size as the Fermi momentum  $k_{f0} = 263 \text{ MeV} \simeq 2m_\pi$  at nuclear matter saturation density. Therefore pions and  $\Delta$ -isobars should both be treated as explicit degrees of freedom in the nuclear many-body problem. It has been found in ref.[10] that the inclusion of the chiral  $\pi N \Delta$  dynamics significantly improves e.g. the momentum-dependence of the (real) single-particle potential  $U(p, k_f)$  and the isospin properties (as revealed by the density-dependent asymmetry energy  $A(k_f)$  and the neutron matter equation of state). Moreover, it guarantees spin-stability of nuclear matter [12].

The purpose of the present paper is to investigate the in-medium chiral condensate (beyond the linear density approximation) in this extended and improved framework for nuclear matter where interaction effects are (almost) exclusively given by one- and two-pion exchange according to the rules of chiral symmetry. Since the pion mass  $m_\pi$  appears as an explicit variable in our calculation we can also study how the "dropping" in-medium condensate evolves from the chiral limit,  $m_\pi = 0$ , to the real world with its fixed amount of explicit chiral symmetry breaking,  $m_\pi = 135 \text{ MeV}$ . We find that the in-medium condensate behaves very differently in both cases,

with drastic consequences for nuclear physics in the chiral limit.

Our starting point is the Feynman-Hellmann theorem which relates the in-medium quark condensate  $\langle \bar{q}q \rangle(\rho)$  to the quark mass derivative of the energy density of isospin-symmetric spin-saturated nuclear matter. Using the Gell-Mann-Oakes-Renner relation  $m_\pi^2 f_\pi^2 = -m_q \langle 0 | \bar{q}q | 0 \rangle$  one finds for the ratio of the in-medium to the vacuum quark condensate:

$$\frac{\langle \bar{q}q \rangle(\rho)}{\langle 0 | \bar{q}q | 0 \rangle} = 1 - \frac{\rho}{f_\pi^2} \left\{ \frac{\sigma_N}{m_\pi^2} \left( 1 - \frac{3k_f^2}{10M_N^2} + \frac{9k_f^4}{56M_N^4} \right) + D(k_f) \right\}, \quad (1)$$

with the Fermi momentum  $k_f$  related to the nucleon density  $\rho = 2k_f^3/3\pi^2$  in the usual way. The term proportional to  $\sigma_N = \langle N | m_q \bar{q}q | N \rangle = m_q \partial M_N / \partial m_q$  comes from the noninteracting Fermi gas including kinetic energy contributions expanded up to order  $M_N^{-3}$ . Interaction contributions beyond the linear density approximation are collected in the function:

$$D(k_f) = \frac{1}{2m_\pi} \frac{\partial \bar{E}(k_f)}{\partial m_\pi}, \quad (2)$$

defined as the derivative of the interaction energy per particle  $\bar{E}(k_f)$  with respect to  $m_\pi^2$ . We mention here that  $f_\pi$  denotes the pion decay constant in the chiral limit and  $m_\pi^2$  stands for the leading linear term in the quark mass expansion of the squared pion mass. With this convention the Gell-Mann-Oakes-Renner relation,  $m_\pi^2 f_\pi^2 = -m_q \langle 0 | \bar{q}q | 0 \rangle$ , becomes exact and  $\langle 0 | \bar{q}q | 0 \rangle$  is the vacuum condensate in the chiral limit.

## 2 Pion mass derivative of the interaction energy

In this section we present analytical expressions for the contributions to the derivative function  $D(k_f)$  as given by various one- and two-pion exchange diagrams. Taking the  $m_\pi^2$ -derivative is a straightforward procedure since we can borrow here heavily from the explicit expressions for the diagrammatic contributions to  $\bar{E}(k_f)$  written down in our previous works [9, 10].

### 2.1 One-pion exchange Fock term

We are working to three-loop order in the energy density. At that order one encounters also pion-loop corrections to the pion-nucleon vertex. As a consequence, the  $1\pi$ -exchange Fock term, eq.(6) in ref.[9], needs to be multiplied by the following renormalization factor:

$$\begin{aligned} \Gamma(m_\pi) = & 1 + \frac{g_A^2 m_\pi^2}{(2\pi f_\pi)^2} \left[ 4\gamma + 1 - 2 \ln \frac{m_\pi}{\lambda} \right] + \frac{g_A^2}{3\pi^2 f_\pi^2} \left\{ \frac{\pi m_\pi^3}{\Delta} - \frac{m_\pi^2}{2} \right. \\ & \left. + (3m_\pi^2 - 2\Delta^2) \ln \frac{m_\pi}{2\Delta} - \frac{2}{\Delta} (\Delta^2 - m_\pi^2)^{3/2} \ln \frac{\Delta + \sqrt{\Delta^2 - m_\pi^2}}{m_\pi} \right\} \\ & + \frac{9g_A^2}{(4\pi f_\pi)^2} \left\{ m_\pi^2 + (4\Delta^2 - 2m_\pi^2) \ln \frac{m_\pi}{2\Delta} + 4\Delta \sqrt{\Delta^2 - m_\pi^2} \ln \frac{\Delta + \sqrt{\Delta^2 - m_\pi^2}}{m_\pi} \right\}, \quad (3) \end{aligned}$$

with  $g_A$  the nucleon axial vector coupling constant in the chiral limit. The last two terms, depending on the delta-nucleon mass splitting  $\Delta = 293$  MeV, arise from pion-loop diagrams involving the  $\Delta(1232)$ -isobar. The low-energy constant  $\gamma(\lambda)$  takes care of the (empirical) Goldberger-Treiman discrepancy. It is determined for any choice of the regularization scale  $\lambda$  by the condition  $(g_{\pi N}/M_N)_{\text{phys}} = \sqrt{\Gamma(m_\pi)} g_A/f_\pi$ , where "phys" denotes physical values.

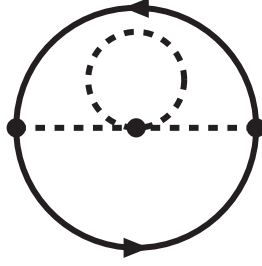


Fig. 1: One-pion exchange Fock diagram with pion selfenergy. Its combinatoric factor is  $1/4$ .

The  $1\pi$ -exchange Fock diagram (with unrenormalized coupling constant) including the relativistic  $1/M_N^2$ -correction leads to the expression:

$$D(k_f)^{(1\pi)} = \frac{9g_A^2 m_\pi}{(8\pi f_\pi)^2} \left\{ \frac{1}{2u} - u + 2 \arctan 2u - \frac{1+8u^2}{8u^3} \ln(1+4u^2) + \frac{m_\pi^2}{15M_N^2} \right. \\ \left. \times \left[ \frac{1}{u} + \frac{21u}{2} + \frac{20u^3}{3} - \left( \frac{25}{4} + 9u^2 \right) \arctan 2u - \frac{1}{4u^3} \ln(1+4u^2) \right] \right\}, \quad (4)$$

where we have introduced the useful dimensionless variable  $u = k_f/m_\pi$ . For reasons of consistency with the loop expansion the renormalization factor  $\Gamma(m_\pi) = 1 + \mathcal{O}(m_\pi^2)$  must be applied only to the static term in eq.(4), and the  $m_\pi^2$ -derivative of  $\Gamma(m_\pi)$  must be multiplied only with the static  $1\pi$ -exchange energy per particle. The necessity for this procedure will become clear in subsection 2.6 when discussing the chiral limit  $m_\pi \rightarrow 0$ .

The loop diagram with a tadpole on the exchanged pion (see Fig. 1) generates a momentum-independent pion selfenergy (i.e. a pion mass shift). Its contribution to the function  $D(k_f)$  reads:

$$D(k_f)^{(\pi\text{-self})} = \frac{9g_A^2 m_\pi^3}{4(4\pi f_\pi)^4} \left\{ \left( 32\pi^2 l_3^r + \ln \frac{m_\pi}{\lambda} \right) \left[ \frac{2}{u} - 2u + 5 \arctan 2u - \frac{1+6u^2}{2u^3} \ln(1+4u^2) \right] \right. \\ \left. + \frac{1}{4u} - \frac{u}{2} + \arctan 2u - \frac{1+8u^2}{16u^3} \ln(1+4u^2) \right\}, \quad (5)$$

with the low-energy constant  $l_3^r(\lambda)$  determined by the relation  $\bar{l}_3 = -64\pi^2 l_3^r(\lambda) - 2 \ln(m_\pi/\lambda) \simeq 3$  [13]. Although this contribution is very small it has to be kept for reasons of consistency.

## 2.2 Iterated one-pion exchange

The Hartree diagram from iterated  $1\pi$ -exchange with two medium insertions (see Fig. 3 and eq.(7) in ref.[9]) leads to the expression:

$$D(k_f)^{(it,H2)} = \frac{3\pi g_A^4 M_N m_\pi^2}{5(4\pi f_\pi)^4} \left\{ \frac{63}{8u} - \frac{193u}{4} + (60 + 16u^2) \arctan 2u - \frac{7}{32u^3} (9 + 100u^2) \ln(1+4u^2) \right\}, \quad (6)$$

and the corresponding Fock diagram with two medium insertions gives:

$$D(k_f)^{(it,F2)} = \frac{3\pi g_A^4 M_N m_\pi^2}{(4\pi f_\pi)^4 u^3} \int_0^u dx \frac{x(u-x)^2(2u+x)}{(1+2x^2)^2} \left[ (2+8x^2+16x^4) \right. \\ \left. \times (\arctan x - \arctan 2x) + 12x^3 + 4x + \frac{x}{1+x^2} \right]. \quad (7)$$

In our way of organizing the many-body calculation, the Pauli blocking corrections are represented by diagrams with three medium insertions. The contribution of the Hartree diagram

with three medium insertions to the function  $D(k_f)$  can be reduced to a one-parameter integral:

$$\begin{aligned}
D(k_f)^{(it,H3)} &= \frac{9g_A^4 M_N m_\pi^2}{(4\pi f_\pi)^4 u^3} \int_0^u dx \left[ 2ux + (u^2 - x^2) \ln \frac{u+x}{u-x} \right] \left\{ 4x(x-u) - \frac{x^2}{1+4x^2} \right. \\
&\quad + \frac{u(x+u)}{2[1+(u+x)^2]} + \frac{u(x-u)}{2[1+(u-x)^2]} + (x^2 - u^2 - 3) \ln \frac{1+(u+x)^2}{1+(u-x)^2} \\
&\quad \left. + 3 \ln(1+4x^2) + \frac{15x}{2} [\arctan(u+x) + \arctan(u-x) - \arctan 2x] \right\}. \quad (8)
\end{aligned}$$

On the other hand, one gets from the Fock diagrams with three medium insertions:

$$\begin{aligned}
D(k_f)^{(it,F3)} &= \frac{9g_A^4 M_N m_\pi^2}{(4\pi f_\pi)^4 u^3} \int_0^u dx \left\{ \frac{G}{8} \left[ 3G - x \frac{\partial G}{\partial x} - u \frac{\partial G}{\partial u} \right] + \frac{x^2}{2} \int_{-1}^1 dy \int_{-1}^1 dz \right. \\
&\quad \left. \times \frac{yz \theta(y^2 + z^2 - 1)}{|yz| \sqrt{y^2 + z^2 - 1}} \left[ \frac{s^2}{1+s^2} - \ln(1+s^2) \right] [\ln(1+t^2) - t^2] \right\}, \quad (9)
\end{aligned}$$

where we have introduced the auxiliary function:

$$G(x, u) = u(1 + u^2 + x^2) - \frac{1}{4x} [1 + (u+x)^2][1 + (u-x)^2] \ln \frac{1 + (u+x)^2}{1 + (u-x)^2}, \quad (10)$$

and the abbreviations  $s = xy + \sqrt{u^2 - x^2 + x^2 y^2}$  and  $t = xz + \sqrt{u^2 - x^2 + x^2 z^2}$ . Note that the expressions in eqs.(6-9) carry the large scale enhancement factor  $M_N$ . It stems from the energy denominator of these iterated diagrams which is proportional to the difference of small nucleon kinetic energies.

## 2.3 Irreducible two-pion exchange

The irreducible two-pion exchange with only nucleons in the intermediate state leads to the following contribution:

$$\begin{aligned}
D(k_f)^{(2\pi)} &= \frac{m_\pi^3}{(4\pi f_\pi)^4} \left\{ \left[ \frac{3}{8u^3} (43g_A^4 + 6g_A^2 - 1) + \frac{9}{4u} (23g_A^4 + 2g_A^2 - 1) \right] \ln^2(u + \sqrt{1+u^2}) \right. \\
&\quad + \left[ u^2(7g_A^4 - 6g_A^2 - 1) - 4 - 6g_A^2 + 46g_A^4 + \frac{3}{4u^2} (1 - 6g_A^2 - 43g_A^4) \right] \sqrt{1+u^2} \\
&\quad \times \ln(u + \sqrt{1+u^2}) + \frac{3}{8u} (43g_A^4 + 6g_A^2 - 1) + \frac{u}{8} (47 + 30g_A^2 - 653g_A^4) \\
&\quad \left. + \frac{u^3}{4} (5 + 22g_A^2 - 19g_A^4) + u^3 (15g_A^4 - 6g_A^2 - 1) \ln \frac{m_\pi}{\lambda} \right\}, \quad (11)
\end{aligned}$$

as obtained by differentiating eq.(14) in ref.[9] with respect to  $m_\pi^2$  at fixed  $k_f$ . We have arranged the  $u^3$ -terms in the last line such that the low-density expansion of eq.(11) starts as  $k_f^3 [\ln(m_\pi/\lambda) + 1/2]$  with no further additive (regularization-scheme dependent) constant to the chiral logarithm. Or stated differently, the underlying  $2\pi$ -exchange interaction at zero momentum transfer has been restricted to the non-analytical piece proportional to  $m_\pi^2 \ln(m_\pi/\lambda)$ . The dependence of the contribution in eq.(11) on the regularization scale  $\lambda$  will be discussed in section 3.2.

## 2.4 Two-pion exchange with virtual $\Delta$ -isobar excitation

We give first the three-body contributions. The Hartree diagram (see Fig. 2 and eq.(5) in ref.[10]) leads to the following closed form expression:

$$D(k_f)^{(\Delta,H3)} = \frac{3g_A^4 m_\pi^4}{\Delta (2\pi f_\pi)^4} \left\{ u^2 - u^4 + \frac{5u^3}{2} \arctan 2u - \frac{1+6u^2}{4} \ln(1+4u^2) \right\}, \quad (12)$$

while the contribution of the Fock diagrams can be represented as a one-parameter integral:

$$D(k_f)^{(\Delta, F3)} = \frac{3g_A^4 m_\pi^4}{4\Delta(4\pi f_\pi)^4 u^3} \int_0^u dx \left\{ 2G_S \left( x \frac{\partial G_S}{\partial x} + u \frac{\partial G_S}{\partial u} - 4G_S \right) + G_T \left( x \frac{\partial G_T}{\partial x} + u \frac{\partial G_T}{\partial u} - 4G_T \right) \right\}, \quad (13)$$

with the two auxiliary functions  $G_S(x, u)$  and  $G_T(x, u)$  written down explicitly in eqs.(7,8) of ref.[10]. As in our previous works we use the value  $3/\sqrt{2}$  for the ratio between the  $\pi N\Delta$ - and  $\pi NN$ -coupling constants.

The two-body terms from  $2\pi$ -exchange with virtual  $\Delta$ -excitations fall into two classes: the dominant terms scaling reciprocally with the mass splitting  $\Delta = 293$  MeV, and the remaining ones with a more complicated  $\Delta$ -dependence. The contribution of the dominant two-body terms to the function  $D(k_f)$  can be written again in closed form:

$$D(k_f)^{(\Delta 2)} = \frac{3\pi g_A^4 m_\pi^4}{70\Delta(2\pi f_\pi)^4} \left\{ (70 + 14u^2 + 3u^4) \arctan u - \frac{43 + 161u^2}{4u^3} \ln(1 + u^2) + \frac{43}{4u} - \frac{281u}{8} - \frac{437u^3}{6} \right\}. \quad (14)$$

It has been derived from the following isoscalar central and isovector tensor one-loop NN-scattering amplitudes [11]:

$$V_C(q) = \frac{3g_A^4}{32\pi f_\pi^4 \Delta} \left\{ \frac{(2m_\pi^2 + q^2)^2}{2q} \arctan \frac{q}{2m_\pi} + m_\pi q^2 + 4m_\pi^3 \right\}, \quad (15)$$

$$W_T(q) = \frac{g_A^4}{128\pi f_\pi^4 \Delta} \left\{ \frac{4m_\pi^2 + q^2}{2q} \arctan \frac{q}{2m_\pi} + m_\pi \right\}, \quad (16)$$

with  $q$  the momentum transfer between the two nucleons. In these expressions we have kept the polynomial pieces proportional to odd powers of the pion mass  $m_\pi$ . These non-analytic terms in the quark mass  $m_q$  are a unique feature of the chiral pion-loop dynamics. For the remaining two-body terms we employ the spectral-function representation [10] and differentiate directly the imaginary parts of the  $\pi N\Delta$ -loop functions with respect to  $m_\pi^2$ . This gives:

$$D(k_f)^{(\Delta 2')} = \frac{3g_A^2}{(4\pi f_\pi)^4} \int_{2m_\pi}^\infty d\mu \left[ 3\mu k_f - \frac{4k_f^3}{3\mu} - \frac{\mu^3}{2k_f} - 4\mu^2 \arctan \frac{2k_f}{\mu} + \frac{\mu^3}{8k_f^3} (12k_f^2 + \mu^2) \right. \\ \times \ln \left( 1 + \frac{4k_f^2}{\mu^2} \right) \left. \left\{ \left[ \frac{2\Delta}{\mu} + \frac{g_A^2}{8\mu\Delta} (8\Delta^2 + 40m_\pi^2 - 13\mu^2) \right] \arctan \frac{\sqrt{\mu^2 - 4m_\pi^2}}{2\Delta} - \frac{g_A^2 \mu m_\pi^2}{\Delta^2 \sqrt{\mu^2 - 4m_\pi^2}} + \sqrt{\mu^2 - 4m_\pi^2} \left[ \frac{3g_A^2 \mu (m_\pi^2 - \Delta^2)}{(\mu^2 + 4\Delta^2 - 4m_\pi^2)^2} - \frac{2 + g_A^2}{2\mu} \right. \right. \right. \\ \left. \left. \left. + \frac{2g_A^2 \mu (m_\pi^2 - \Delta^2) - \mu \Delta^2}{2\Delta^2 (\mu^2 + 4\Delta^2 - 4m_\pi^2)} \right] \right\} \right\}, \quad (17)$$

where the  $g_A^2$ -terms in the curly bracket stem from box diagrams and the  $g_A$ -independent ones from the triangle diagram. The spectral-function representation in eq.(17) involves one subtraction of a term linear in density  $\rho = 2k_f^3/3\pi^2$ . The associated subtraction constant receives also contributions from the pion loop diagrams with a non-analytical dependence on the quark mass. We reinstate these distinguished pieces from the chiral pion-loop dynamics by the additional contribution linear in density:

$$D(k_f)^{(dt)} = \frac{3g_A^2 k_f^3}{(4\pi f_\pi)^4} \left\{ (2 - 5g_A^2) \ln \frac{m_\pi}{2\Delta} + \frac{4\Delta^2 - 5g_A^2(2\Delta^2 + 3m_\pi^2)}{2\Delta \sqrt{\Delta^2 - m_\pi^2}} \ln \frac{\Delta + \sqrt{\Delta^2 - m_\pi^2}}{m_\pi} \right\}, \quad (18)$$

which has the property that it vanishes in the chiral limit.

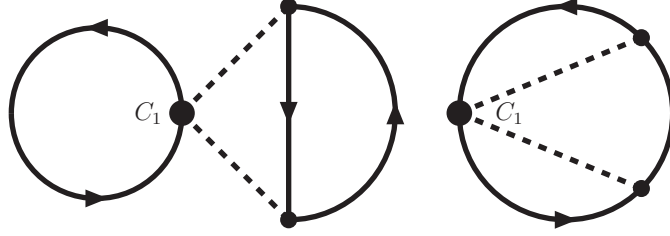


Fig. 2: Hartree and Fock diagrams related to the chiral  $\pi\pi NN$  contact vertex proportional to  $c_1$ . The combinatoric factors of these diagrams are  $1/2$  and  $1$ , in the order shown.

## 2.5 Chiral $\pi\pi NN$ contact vertex proportional to $c_1$

In chiral perturbation theory the nucleon sigma-term  $\sigma_N$  has a specific nonlinear dependence on the quark mass  $m_q$ . The leading linear term comes from the effective Lagrangian  $\mathcal{L}_{\pi N}^{(2)} = c_1 \bar{N} N \text{tr} \chi_+ = 4c_1 m_\pi^2 \bar{N} N \sqrt{1 - \vec{\pi}^2/f_\pi^2}$  and the nonlinearities arise from pion-loops and higher order counterterms. Putting together all (numerically) relevant pieces the ratio  $\sigma_N/m_\pi^2$  entering eq.(1) takes the form:

$$\begin{aligned} \frac{\sigma_N}{m_\pi^2} = & -4c_1 - \frac{9g_A^2 m_\pi}{64\pi f_\pi^2} + \frac{3c_1 m_\pi^2}{2\pi^2 f_\pi^2} \ln \frac{m_\pi}{\lambda} \\ & + \frac{9g_A^2}{(4\pi f_\pi)^2} \left\{ \Delta \ln \frac{m_\pi}{2\Delta} + \sqrt{\Delta^2 - m_\pi^2} \ln \frac{\Delta + \sqrt{\Delta^2 - m_\pi^2}}{m_\pi} \right\}. \end{aligned} \quad (19)$$

By chiral symmetry, the  $c_1$ -term in the effective Lagrangian generates also an additional  $\pi\pi NN$ -contact interaction with vertex insertion:  $-4ic_1 m_\pi^2 f_\pi^{-2} \delta^{ab}$ . On the one hand it makes up the sizeable logarithmic loop correction to  $\sigma_N/m_\pi^2$  in eq.(19). On the other hand it gives rise to an additional two-pion exchange contribution to the NN-interaction, and moreover it generates a long-range three-nucleon force (see diagrams in Fig. 2). The two-body terms in nuclear matter lead to the following contribution to the  $m_\pi^2$ -derivative of the energy per particle:

$$D(k_f)^{(c_1,2)} = \frac{3g_A^2 c_1 m_\pi^4}{280\pi^3 f_\pi^4} \left\{ (14u^2 + 3u^4) \arctan u + \frac{27 + 49u^2}{4u^3} \ln(1 + u^2) - \frac{27}{4u} - \frac{71u}{8} - \frac{99u^3}{2} \right\}, \quad (20)$$

which has been derived from the isoscalar central one-loop NN-scattering amplitude:

$$V_C(q) = \frac{3g_A^2 c_1 m_\pi^2}{4\pi f_\pi^4} \left\{ \frac{2m_\pi^2 + q^2}{2q} \arctan \frac{q}{2m_\pi} + m_\pi \right\}. \quad (21)$$

In addition, there are  $c_1$ -contributions from the three-body Hartree diagram:

$$D(k_f)^{(c_1,H3)} = \frac{3g_A^2 c_1 m_\pi^4}{(2\pi f_\pi)^4} \left\{ 3u^2 - 2u^4 + 6u^3 \arctan 2u - \left( \frac{3}{4} + 4u^2 \right) \ln(1 + 4u^2) \right\}, \quad (22)$$

and the three-body Fock diagram:

$$D(k_f)^{(c_1,F3)} = \frac{9g_A^2 c_1 m_\pi^4}{(4\pi f_\pi)^4 u^3} \int_0^u dx G \left[ 4G - x \frac{\partial G}{\partial x} - u \frac{\partial G}{\partial u} \right], \quad (23)$$

with the auxiliary function  $G(x, u)$  defined in eq.(10).

## 2.6 Chiral limit

The  $m_\pi^2$ -derivative of the energy per particle,  $D(k_f)$ , presented in the previous subsections takes a particularly simple form in the chiral limit  $m_\pi = 0$ . In that limiting case almost all integrals can be solved and the dependence on the Fermi momentum  $k_f$  becomes simply powerlike (with an exponent determined by the mass dimension of the prefactor). The subscript 0 denotes the function  $D(k_f)$  in the chiral limit  $m_\pi \rightarrow 0$ . The  $1\pi$ -exchange Fock term (with the renormalization factor in the chiral limit,  $\Gamma(0) = 1$ ) gives:

$$D_0(k_f)^{(1\pi)} = \frac{g_A^2 k_f}{(4\pi f_\pi)^2} \left( \frac{k_f^2}{M_N^2} - \frac{9}{4} \right), \quad (24)$$

and the total contribution from iterated  $1\pi$ -exchange reads:

$$D_0(k_f)^{(\text{it})} = \frac{g_A^4 M_N k_f^2}{5(4\pi f_\pi)^4} (8\pi^2 + 36 \ln 2 - 3). \quad (25)$$

The contribution from irreducible  $2\pi$ -exchange:

$$D_0(k_f)^{(2\pi)} = \frac{k_f^3}{(4\pi f_\pi)^4} \left\{ (g_A^2 - 1)(7g_A^2 + 1) \ln \frac{2k_f}{\lambda} + \frac{1}{4}(5 + 22g_A^2 - 19g_A^4) + 8g_A^4 \ln \frac{m_\pi}{\lambda} \right\}, \quad (26)$$

has a logarithmic singularity  $\ln(m_\pi/\lambda)$ . It gets exactly canceled by the  $m_\pi^2$ -derivative of the renormalization factor  $\Gamma(m_\pi)$  applied to the static  $1\pi$ -exchange:

$$D_0(k_f)^{(\text{ren})} = \frac{k_f^3}{(2\pi f_\pi)^4} \left\{ g_A^4 \left( \gamma - \frac{1}{2} \ln \frac{m_\pi}{\lambda} \right) + C \right\}. \quad (27)$$

This crucial feature instructs us that one must work consistently with the parameters in the chiral limit as they are given by the effective chiral Lagrangian. It is mandatory to include only those renormalization effects to physical parameters which are actually generated by the pion-loops to the order one is working. The constant  $C$  represents the additional effect of a NN-contact coupling linear in the quark mass  $m_q$ , and  $\gamma$  is a left-over from the Goldberger-Treiman discrepancy. The two- and three-body terms from  $2\pi$ -exchange with single  $\Delta$ -excitation scaling as  $1/\Delta$  read together:

$$D_0(k_f)^{(\Delta 3)} = \frac{g_A^4 k_f^4}{\Delta (4\pi f_\pi)^4} \left( \frac{12\pi^2}{35} - 25 \right), \quad (28)$$

where the two-body term eq.(14) has contributed  $36\pi^2/35$  to the numerical factor in brackets. For the remaining two-body Fock terms from  $2\pi$ -exchange with  $\Delta$ -excitations the spectral-function representation turns into:

$$D_0(k_f)^{(\Delta 2')} = \frac{g_A^2 \Delta^3}{(4\pi f_\pi)^4} \int_0^\infty dx x \left\{ g_A^2 \left[ \frac{2x + 11x^3 + 6x^5}{(1+x^2)^2} + (13x^2 - 2) \arctan x \right] + \frac{4x + 6x^3}{1+x^2} - 4 \arctan x \right\} \Phi \left( \frac{k_f}{x\Delta} \right), \quad (29)$$

with the auxiliary function:

$$\Phi(y) = \frac{6}{y} - 9y + y^3 + 24 \arctan y - \frac{6}{y^3} (1 + 3y^2) \ln(1 + y^2). \quad (30)$$

For low densities the contribution in eq.(29) behaves as  $k_f^5 \ln(k_f/\Delta)$ . Finally, the total contribution from the  $\pi\pi NN$ -contact vertex proportional to  $c_1$  reads, in the chiral limit:

$$D_0(k_f)^{(c_1)} = \frac{3g_A^2 c_1 k_f^4}{(2\pi f_\pi)^4} \left( \frac{\pi^2}{35} - \frac{5}{4} \right). \quad (31)$$

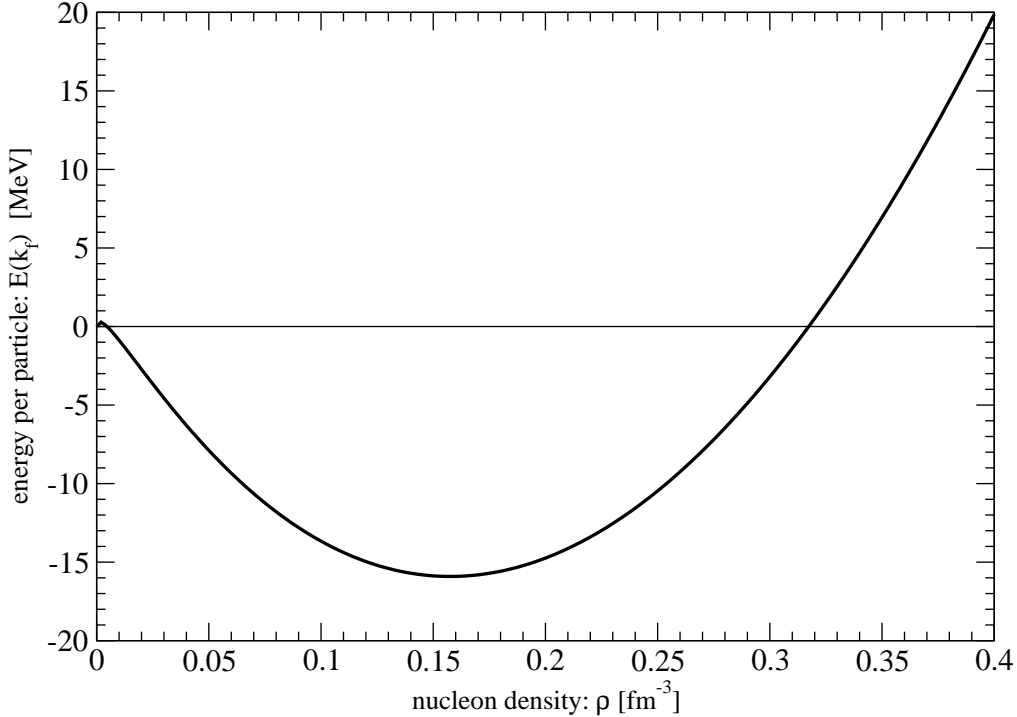


Fig. 3: The nuclear matter saturation curve underlying our calculation of the in-medium quark condensate. Apart from the interaction contributions described in refs.[9, 10] and those proportional to  $c_1$ , it includes one single adjusted term linear in density,  $\bar{E}(k_f)^{(\text{adj})} = -7.64 \text{ GeV}^{-2} k_f^3$ .

### 3 Results

This section presents and discusses results for the in-medium chiral condensate as a function of baryon density  $\rho$ . Apart from just collecting and computing the series of terms given in section 2, this includes also a detailed investigation of the pion mass dependence of the quark condensate at given density  $\rho$ . It is furthermore necessary to estimate the quark mass dependence of the NN-contact term (i.e. the size of the parameter  $C$  introduced in eq.(27)) which encodes short-distance dynamics not controlled by the underlying chiral effective field theory. At this point we can now take very recent computations of the NN-potential from lattice QCD for orientation.

#### 3.1 Parameter fixing

First, we have to fix the parameters. The pion decay constant in the chiral limit  $f_\pi$  is determined by the relation:  $f_{\pi,\text{phys}} = f_\pi[1 + \bar{l}_4(m_\pi/4\pi f_\pi)^2] = 92.4 \text{ MeV}$ . Choosing the central value  $\bar{l}_4 = 4.4 \pm 0.2$  of ref.[13] one gets  $f_\pi = 86.5 \text{ MeV}$ . For the nucleon axial vector coupling constant  $g_A$  in the chiral limit we take the value  $g_A = 1.224$  as obtained recently via chiral extrapolations of lattice data in ref.[14]. A similar analysis [15] gives for the nucleon mass in the chiral limit  $M_N = 882 \text{ MeV}$  and for the low-energy constant  $c_1 = -0.93 \text{ GeV}^{-1}$  (as central values). For the delta-nucleon mass splitting we take the empirical value  $\Delta = 293 \text{ MeV}$ . This is consistent to the order in the loop expansion we are working here. The parameter  $\gamma$  introduced in eq.(3) is determined by the relation:  $(g_{\pi N}/M_N)_{\text{phys}} = \sqrt{\Gamma(m_\pi)} g_A/f_\pi$ . Taking for the left hand side  $13.2/(939 \text{ MeV})$ , we deduce  $\gamma = -1.505$  at the regularization scale  $\lambda = M_N = 882 \text{ MeV}$ . Or stated differently, for our choice of parameters ( $g_A$  and  $f_\pi$  in the chiral limit) the Goldberger-Treiman relation is exact within one percent. We neglect the 1.2%-difference between the physical pion mass  $m_{\pi,\text{phys}} = m_\pi[1 - \bar{l}_3(m_\pi/8\pi f_\pi)^2]$  (with  $\bar{l}_3 \simeq 3$  [13]) and the leading order one,

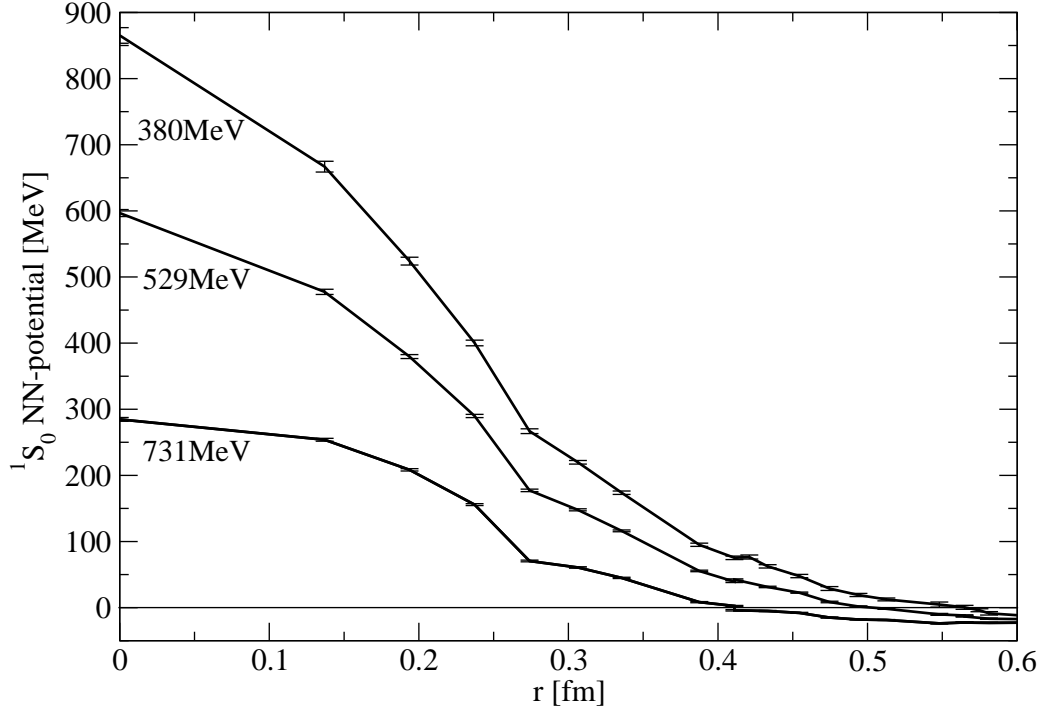


Fig. 4: The nucleon-nucleon potential in the  $^1S_0$  channel from lattice QCD [16] for three different pion masses,  $m_\pi = (380, 529, 731) \text{ MeV}$ .

$m_\pi$ , since this difference is much smaller than the splitting between charged and neutral pion masses.

With these fixed parameters we obtain (for the physical value of the pion mass  $m_\pi = 135 \text{ MeV}$ ) the nuclear matter equation of state as shown in Fig.3. Besides the  $1\pi$ - and  $2\pi$ -exchange contributions described in refs.[9, 10] and those proportional to  $c_1$ , it includes one single adjusted term linear in density:  $\bar{E}(k_f)^{(\text{adj})} = -7.64 \text{ GeV}^{-2} k_f^3$ . We interpret its strength parameter to subsume all unresolved short-distance NN-dynamics relevant for nuclear matter at low and moderate densities  $0 \leq \rho \leq 2.5\rho_0 = 0.4 \text{ fm}^{-3}$ . Its (weak) implicit quark mass dependence will be estimated below. The nuclear matter compressibility  $K = k_{f0}^2 \bar{E}''(k_{f0})$  related to the curvature of the saturation curve at its minimum comes out as  $K = 295 \text{ MeV}$ . This value lies at the high side of present semi-empirical determinations of  $K$  [17].

Next, we estimate the parameter  $C$  introduced in eq.(27) which represents quark mass dependent effects from the short-range NN-interaction. The simple model of  $\omega(782)$ -meson exchange would give  $C^{(\omega)} \simeq -0.7$ , a large correction, choosing an  $\omega N$ -coupling constant of order 10 and the constituent quark counting rule  $\partial m_\omega / \partial m_q = 2$ . However, since the  $\omega$ -exchange model has no clear connection to the short-range NN-dynamics of QCD, we follow another option. Recently, the nucleon-nucleon potential has been studied within lattice QCD [16] using the quenched approximation. The short-distance part ( $r \leq 0.6 \text{ fm}$ ) of this potential in the  $^1S_0$  channel is shown in Fig.4 for three different pion masses,  $m_\pi = (380, 529, 731) \text{ MeV}$ . We can identify the volume integrals  $I_0 = 4\pi \int_0^{r_0} dr r^2 V(r)$  over the repulsive cores of these potentials with the strength of a contact-coupling in the  $^1S_0$  channel. From the three values  $I_0 = (83.6, 53.3, 21.9) \text{ MeVfm}^3$  we obtain a mean value for the derivative with respect to the squared pion mass:  $\partial I_0 / \partial m_\pi^2 \simeq -0.17 \text{ GeV}^{-1} \text{fm}^3$ . Via the contribution  $\bar{E}(k_f)^{(\text{sd})} = I_0 k_f^3 / 4\pi^2$  to the energy per particle we estimate the parameter  $C$  as  $C = 4\pi^2 f_\pi^4 \partial I_0 / \partial m_\pi^2 \simeq -0.05$ . In comparison to the  $\omega$ -meson exchange this is a rather small number. These considerations raise also some doubts concerning the significance of the vector boson exchange phenomenology as a valid picture of the short-distance NN-dynamics. Even with a factor 2, to include an equally

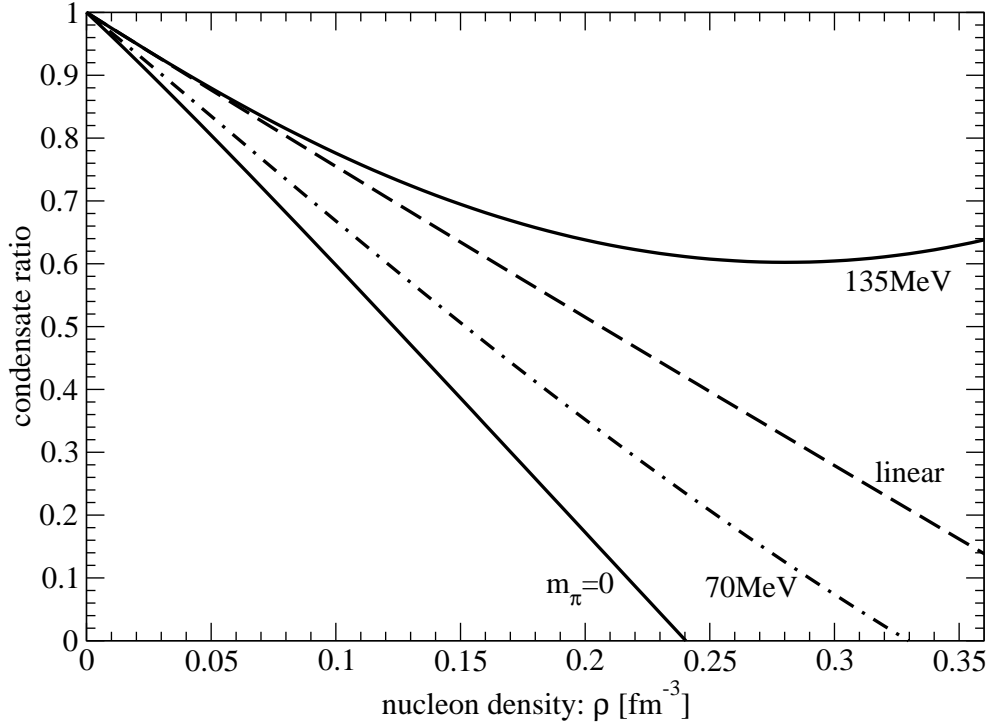


Fig. 5: The ratio of the in-medium chiral condensate to its vacuum value as a function of the nucleon density  $\rho$  for three different values of the pion mass,  $m_\pi = (0, 70, 135)$  MeV. The dashed line corresponds to the linear density approximation using the empirical central value  $\sigma_N = 45$  MeV [4].

strong contribution from the  ${}^3S_1$  channel [16], the value  $C \simeq -0.1$  affects the condensate ratio at nuclear matter saturation density  $\rho_0 = 0.16 \text{ fm}^{-3}$  (corresponding to  $k_{f0} = 263$  MeV) only at the 3 permille level (and 4 times as much at  $2\rho_0$ ).

We can therefore conclude that the short-range NN-dynamics as given by lattice QCD [16] has a negligible influence on the in-medium chiral condensate  $\langle \bar{q}q \rangle(\rho)$ . The deviations from the linear density approximation are primarily caused by the long- and intermediate range  $1\pi$ - and  $2\pi$ -exchange dynamics.

There is some residual dependence on the regularization scale  $\lambda$  left over which is not balanced by the parameters  $l_3^r(\lambda)$  and  $\gamma(\lambda)$  (namely from the last term in eq.(11)).<sup>2</sup> Varying  $\lambda$  between 0.6 GeV and 1.2 GeV changes the condensate ratio at  $\rho_0$  by 3.5%. Since this is much smaller than the effect induced by the uncertainty of the empirical nucleon sigma-term  $\sigma_N = (45 \pm 8)$  MeV [4] we stay with the "natural" choice of  $\lambda = M_N = 882$  MeV. When inserting into eq.(19) it reproduces correctly  $\sigma_N = 44.3$  MeV for  $m_\pi = 135$  MeV.

### 3.2 In-medium condensate

We are now in the position to present and discuss numerical results for the in-medium quark condensate. Fig.5 shows the condensate ratio  $\langle \bar{q}q \rangle(\rho)/\langle 0|\bar{q}q|0 \rangle$  as a function of the nucleon density  $\rho = 2k_f^3/3\pi^2$  in the region  $0 \leq \rho \leq 0.36 \text{ fm}^{-3} = 2.25\rho_0$  (i.e.  $k_f \leq 345$  MeV) for three different values of the pion mass,  $m_\pi = (0, 70, 135)$  MeV. The dashed line in Fig. 5 corresponds to the linear density approximation using the empirical central value  $\sigma_N = 45$  MeV of the nucleon sigma-term. One observes a very strong and nonlinear dependence of the "dropping"

<sup>2</sup>In principle, this scale dependence is balanced by the parameter  $C(\lambda)$  in eq.(27). But this (formal) point of view introduces the need to fix the scale  $\lambda$  in an estimate of  $C$ .

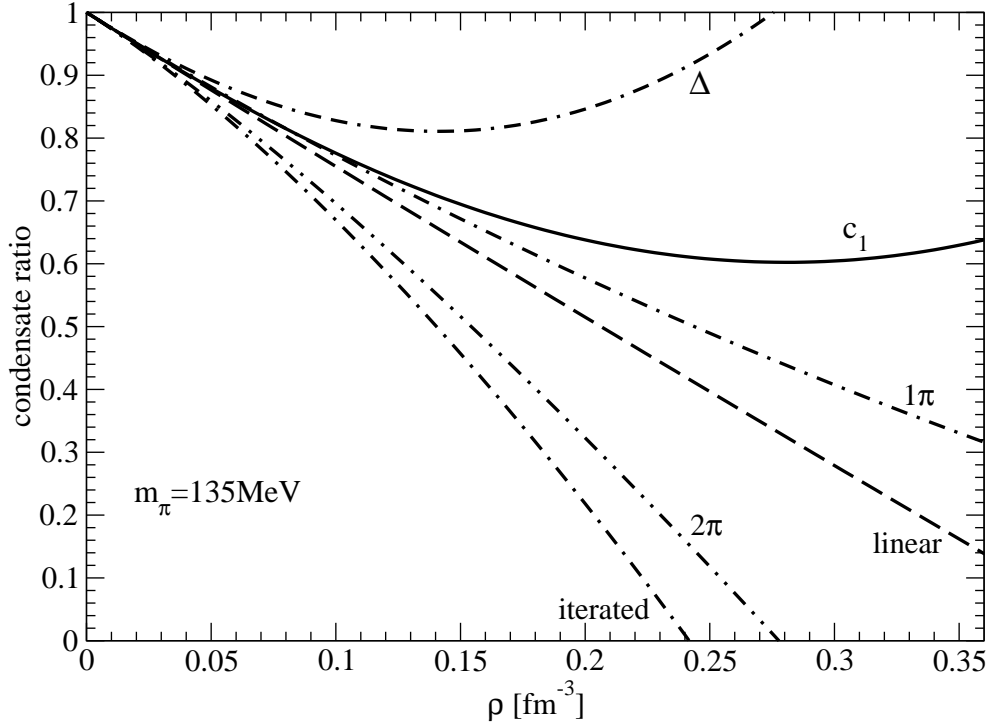


Fig. 6: Interaction contributions to the ratio between in-medium and vacuum chiral condensate. The five classes described in subsections 2.1-2.5 are consecutively added in the sequence: linear  $\rightarrow$   $1\pi$   $\rightarrow$  iterated  $\rightarrow$   $2\pi$   $\rightarrow$   $\Delta$   $\rightarrow$   $c_1$ .

condensate on the actual value of the pion mass  $m_\pi$ . In the chiral limit,  $m_\pi = 0$ , the quark condensate decreases effectively with a slope 1.8 times as large as given by the linear density approximation. As a consequence chiral symmetry would be restored already at about  $1.5\rho_0$  if the up- and down-quark masses were strictly zero. This faster decrease is caused by two features: First, the ratio  $\sigma_N/m_\pi^2 = -4c_1 = 3.72 \text{ GeV}^{-1}$  is, in the chiral limit, about 1.5 times larger than at the physical point,  $45/135^2 \text{ MeV}^{-1} = 2.47 \text{ GeV}^{-1}$ . Secondly, the two-pion exchange effects in the chiral limit drive the condensate ratio further down. Of course, the actual density at which chiral symmetry restoration would occur can only be roughly estimated in our calculation: once the chiral condensate becomes too small the very foundation of the chiral effective field theory approach to nuclear matter (namely the spontaneous breaking of chiral symmetry in the vacuum) is lost.

At the physical value of the pion mass,  $m_\pi = 135 \text{ MeV}$ , the density dependence of the condensate ratio  $\langle\bar{q}q\rangle(\rho)/\langle 0|\bar{q}q|0\rangle$  is drastically different. At densities around  $1.8\rho_0$  the in-medium condensate stabilizes now at about 60% of its vacuum value, and there is no further reduction in the entirely density region where the present chiral approach to nuclear matter can be trusted. For higher values of the pion mass the effects counteracting chiral restoration become even more pronounced.

Let us have a closer look at individual contributions. At  $2\rho_0 = 0.32 \text{ fm}^{-3}$  (corresponding to  $k_f = 331.4 \text{ MeV}$ ) one gets from the sequence of the five classes of interaction contributions (described in subsections 2.1 to 2.5) a total correction to  $\langle\bar{q}q\rangle(\rho)/\langle 0|\bar{q}q|0\rangle$  beyond the linear density approximation of  $(0.14 - 0.83 + 0.27 + 1.34 - 0.54) = 0.38$ . Notice the cancellation between large contributions of opposite signs from iterated  $1\pi$ -exchange and  $2\pi$ -exchange with virtual  $\Delta(1232)$ -excitation. At normal nuclear matter density  $\rho_0 = 0.16 \text{ fm}^{-3}$  the individual entries are about a factor 4 smaller:  $(0.04 - 0.24 + 0.07 + 0.33 - 0.13) = 0.07$ , suggesting an approximate  $\rho^2$ -dependence of the total interaction contribution.

Fig. 6 shows separately the effects of the five classes of interaction contributions. They are consecutively added up in the sequence: *linear*  $\rightarrow 1\pi \rightarrow$  *iterated*  $\rightarrow 2\pi \rightarrow \Delta \rightarrow c_1$ . The last two major steps (in opposite directions) should not be misinterpreted as a sign of bad convergence since the corresponding terms belong to the same order in the small momentum expansion of the nuclear matter energy density ( $-4c_1 \simeq 3g_A^2/4\Delta$ ). Fig. 6 actually demonstrates the prominent importance of the  $2\pi$ -exchange interaction beyond leading order for the in-medium quark condensate.

It is important to include all effects generated by the pion-loops. For example, if one would drop the last constant term proportional to  $4m_\pi^3 \sim m_q^{3/2}$  in eq.(15) an amount of 0.25 would be missing in the total balance (at  $\rho_0$ ). As a consequence of that omission the condensate ratio would lie appreciably below the linear density approximation. This particular non-analytical  $4m_\pi^3$ -term gives also an explanation for the drastically different behavior of the in-medium condensate in the chiral limit and for the physical pion mass. Its contribution to the condensate ratio,  $27g_A^4 m_\pi \rho^2 / (128\pi f_\pi^6 \Delta)$ , vanishes in the chiral limit,  $m_\pi = 0$ , but reaches 100% for the physical pion mass  $m_\pi = 135$  MeV at  $\rho = 0.32 \text{ fm}^{-3} = 2\rho_0$ . This selective consideration does, of course, not mean that the other one- and two-pion exchange contributions would not also depend strongly on the pion mass. Their dependences can be studied easily case by case with the help of the analytical formulas presented in section 2. In general, one can say that the condensate ratio  $\langle \bar{q}q \rangle(\rho) / \langle 0 | \bar{q}q | 0 \rangle$  is affected significantly by interaction terms which otherwise play only a marginal role for the nuclear matter equation of state  $\bar{E}(k_f)$  (as e.g. the chiral  $\pi\pi NN$ -contact term proportional to  $c_1$ ). This pronounced shifting of weights comes from taking the derivative with respect to the squared pion mass  $m_\pi^2$ . On the other hand, the Fermi gas approximation (i.e. the linear density approximation) works reasonably well for the in-medium chiral condensate almost up to nuclear matter saturation density  $\rho_0 = 0.16 \text{ fm}^{-3}$ , even though it is far from correctly describing nuclear matter as a self-bound Fermi liquid.

Let us compare our results for the in-medium chiral condensate with other works which have treated to some limited extent the pion-exchange dynamics in nuclear matter. In the work of Lutz et al. [8]  $1\pi$ -exchange plus an adjustable NN-contact interaction have been iterated to second order. In the region  $0 \leq \rho \leq 2\rho_0$  they find a weaker (positive) deviation from the linear density approximation, with no trend for stabilization of the in-medium condensate. This difference comes from not including the irreducible  $2\pi$ -exchange, the chiral  $\pi N\Delta$ -dynamics and the  $c_1$ -contact vertex. Recently, the Tübingen group [18] has employed the chiral nucleon-nucleon potential at next-to-leading order to calculate nuclear matter within the relativistic Dirac-Brueckner-Hartree-Fock approach. They also derive the in-medium chiral condensate by exploiting the Feynman-Hellmann theorem eq.(1). Irrespective of using the Hartree-Fock or Brueckner-Hartree-Fock approximation, their effects from pion-exchange interactions (e.g.  $\sim 15\%$  at  $2\rho_0$  [18]) are much smaller than in our calculation. Moreover, there is no trend of stabilization in the whole density region  $0 \leq \rho \leq 3\rho_0$  considered. Again, these substantial differences arise in ref.[18] from taking only the next-to-leading order chiral NN-potential (i.e.  $1\pi$ -exchange and irreducible  $2\pi$ -exchange), but neglecting the actually more important effects from  $2\pi$ -exchange with virtual  $\Delta$ -isobar excitation. We note that our perturbative calculation, when truncated to  $1\pi$ -exchange, iterated  $1\pi$ -exchange and irreducible  $2\pi$ -exchange exchange, would lead to an in-medium condensate below the linear density approximation (see Fig. 6). Qualitative differences may also come from the approximations (angle-averaged Pauli-blocking operator, etc.) used in the Brueckner-Hartree-Fock calculation of ref.[18] and not treating the iterated  $1\pi$ -exchange in full detail (as done in the present work). Apart from all these differences, ref.[18] agrees with our conclusion that the short-range NN-dynamics plays only a minor role for the in-medium chiral condensate. It is indicated to repeat the calculation of ref.[18] with the more complete next-to-next-to-leading order chiral NN-potential including the non-analytical polynomial pieces.

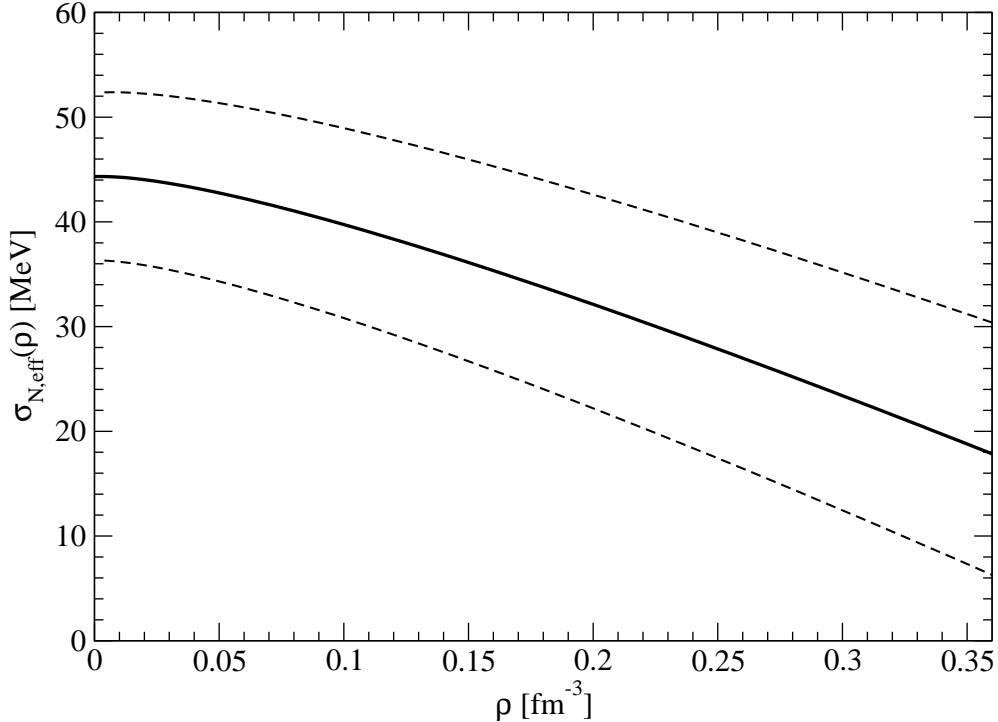


Fig. 7: The effective in-medium nucleon sigma-term  $\sigma_{N,\text{eff}}(\rho)$  versus the nucleon density  $\rho$  with its error band  $\pm 8$  MeV.

Our results for the in-medium chiral condensate can be alternatively summarized by the density dependent effective nucleon sigma-term:

$$\sigma_{N,\text{eff}}(\rho) = \sigma_N \left( 1 - \frac{3k_f^2}{10M_N^2} + \frac{9k_f^4}{56M_N^4} \right) + m_\pi^2 D(k_f). \quad (32)$$

It captures the correlation effects in the nuclear medium which reduce the tendency towards chiral symmetry restoration. Fig. 7 shows the effective nucleon sigma-term<sup>3</sup> as a function of the density for  $0 \leq \rho \leq 0.36 \text{ fm}^{-3}$ . In this figure we display also the uncertainties associated with the still existing error band of  $\pm 8$  MeV in the empirical determination of  $\sigma_N$ . Moreover, we have varied the regularization scale  $\lambda$  between 0.6 GeV and 1.2 GeV which leads to some widening of the error band as the density increases.

## 4 Summary and concluding remarks

In this work we have used in-medium chiral perturbation theory to calculate the quark condensate  $\langle \bar{q}q \rangle(\rho)$  beyond the linear density approximation. The pertinent correction term follows from differentiating the interaction contributions to the energy per particle of isospin-symmetric nuclear matter with respect to the pion mass. Analytical expressions for the contributions to  $D(k_f) = \partial \bar{E}(k_f) / \partial m_\pi^2$  from  $1\pi$ -exchange (with  $m_\pi$ -dependent vertex corrections), iterated  $1\pi$ -exchange and irreducible  $2\pi$ -exchange with inclusion of  $\Delta$ -isobar excitations and Pauli-blocking corrections have been presented in section 2.

We find a strong, nonlinear dependence of the "dropping" in-medium condensate on the value of the pion (or light quark) mass. In the chiral limit,  $m_\pi = 0$ , chiral restoration seems to be reached already at about 1.5 times normal nuclear matter density. By contrast, for the physical

<sup>3</sup>A qualitatively similar result, though based on a different approach, has been reported in ref.[19].

pion mass  $m_\pi = 135$  MeV, the in-medium condensate stabilizes at about 60% of its vacuum value above that same density. Including systematically the effects from  $2\pi$ -exchange with  $\Delta(1232)$ -isobar excitation (or the equivalent chiral  $\pi\pi NN$  contact interactions  $c_{2,3,4}$ ) is crucial in order to obtain such a pronounced behavior. Non-analytical (contact) terms in the quark mass (such as  $m_\pi^3 \sim m_q^{3/2}$ ), which are often dropped in the presentation of the chiral NN-potential, have a very strong influence on the in-medium chiral condensate. Below  $3\rho_0/4 = 0.12$  fm $^{-3}$  the correction beyond the linear density approximation remain relatively small. This finding can be taken as an a posteriori justification of the assumptions made in ref.[20] about the in-medium scalar mean-field.

As a consequence of the hindered tendency towards chiral symmetry restoration (in the real world with  $m_\pi = 135$  MeV), pions and nucleons can be used as effective low-energy degrees of freedom at least up to twice nuclear matter density. The major source of uncertainty for the density dependence of  $\langle\bar{q}q\rangle(\rho)$  is caused by the error band in the empirical determination of the nucleon sigma-term  $\sigma_N = (45 \pm 8)$  MeV. One can hope that upcoming dispersion relation analyses of  $\pi N$ -scattering data and lattice QCD calculations will lead to a more accurate value of  $\sigma_N$ . Of course, there remain also questions about the size of effects from yet higher order interaction contributions related to  $3\pi$ -exchange, two-loop  $2\pi$ -exchange etc. On the other hand, an estimate based on recent lattice QCD results indicates that the short-distance NN-dynamics has only a very small effect on the density dependence of the quark condensate  $\langle\bar{q}q\rangle(\rho)$ .

## Acknowledgments

We thank T. Hatsuda and N. Ishii for providing us with the nucleon-nucleon potential from lattice QCD and for stimulating discussions.

## References

- [1] P. Gerber and H. Leutwyler, *Nucl. Phys.* **B321**, 387 (1989).
- [2] M. Cheng et al., *Phys. Rev.* **D74**, 054507 (2006); hep-lat/0710.0354.
- [3] Y. Aoki, Z. Fodor, S.D. Katz, and K.K. Szabo, *Phys. Lett.* **B643**, 46 (2006).
- [4] J. Gasser, H. Leutwyler and M.E. Sainio, *Phys. Lett.* **B253**, 252 (1991).
- [5] T.D. Cohen, R.J. Furnstahl, and D.K. Griegel, *Phys. Rev.* **C45**, 1881 (1992).
- [6] G.Q. Li and C.M. Ko, *Phys. Lett.* **B338**, 118 (1994).
- [7] R. Brockmann and W. Weise, *Phys. Lett.* **B367**, 40 (1996).
- [8] M. Lutz, B. Friman and C. Appel, *Phys. Lett.* **B474**, 7 (2000).
- [9] N. Kaiser, S. Fritsch and W. Weise, *Nucl. Phys.* **A697**, 255 (2002).
- [10] S. Fritsch, N. Kaiser and W. Weise, *Nucl. Phys.* **A750**, 259 (2005).
- [11] N. Kaiser, S. Gerstendörfer and W. Weise, *Nucl. Phys.* **A637**, 395 (1998).
- [12] N. Kaiser, *Phys. Rev.* **C70**, 054001 (2004).
- [13] G. Colangelo, J. Gasser and H. Leutwyler, *Nucl. Phys.* **B603**, 125 (2001).
- [14] M. Procura, B.U. Musch, T.R. Hemmert, and W. Weise, *Phys. Rev.* **D75**, 014503 (2007).
- [15] M. Procura, B.U. Musch, T. Wollenweber, T.R. Hemmert, and W. Weise, *Phys. Rev.* **D73**, 114510 (2006).
- [16] N. Ishii, S. Aoki, and T. Hatsuda, *Phys. Rev. Lett.* **99**, 022001 (2007); hep-lat/0710.4422.
- [17] D. Vretenar, T. Niksic, and P. Ring, *Phys. Rev.* **C68**, 024310 (2003).
- [18] O. Plohl and C. Fuchs, *Nucl. Phys.* **A**, (2007) in print; nucl-th/0710.3700.
- [19] W. Bentz and A.W. Thomas, *Nucl. Phys.* **A696**, 138 (2001).
- [20] P. Finelli, N. Kaiser, D. Vretenar and W. Weise, *Nucl. Phys.* **A770**, 1 (2006).